Understanding the Interaction of the Porphyrin Macrocycle to Reactive Metal Substrates: Structure, Bonding, and Adatom Capture

Matthew S. Dyer,[†] Abel Robin,[†] Sam Haq,[†] Rasmita Raval,[†] Mats Persson,[†,‡,*] and Jiří Klimeš[§]

[†]The Surface Science Research Center, The University of Liverpool, Liverpool L69 3BX, U.K., [‡]Department of Applied Physics, Chalmers University of Technology, SE-412 96 Göteborg, Sweden, and [§]London Centre for Nanotechnology and Department of Chemistry, University College London, London WC1E 6BT, U.K.

ABSTRACT We investigate the adsorption and conformation of free-base porphines on Cu(110) using STM, reflection absorption infrared spectroscopy, and periodic DFT calculations in order to understand how the central polypyrrole macrocycle, common to all porphyrins, interacts with a reactive metal surface. We find that the macrocycle forms a chemisorption bond with the surface, arising from electron donation into down-shifted and nearly degenerate unoccupied porphine π-orbitals accompanied with electron back-donation from molecular π-orbitals. Our calculations show that van der Waals interactions give rise to an overall increase in the adsorption energy but only minor changes in the adsorption geometry and electronic structure. In addition, we observe copper adatoms being weakly attracted to adsorbed porphines at specific molecular sites. These results provide important insights into porphyrin−surface interactions that, ultimately, will govern the design of robust surface-mounted molecular devices based on this important class of molecules.

KEYWORDS: free-base porphine · molecular adsorption · Cu(110) surface · scanning tunneling microscopy · reflection absorption infrared spectra · density functional calculations · van der Waals interactions

In recent years, there has been a great interest in exploiting porphyrin molecules in engineering functionalized nanostructures on surfaces with potential applications in nanoscience, molecular electronics, and photonics.[1,2] This interest stems from the fact that the porphyrin molecules can be tailored to have a wide variety of magnetic, photochemical, and catalytic properties using a range of substituents and central metal atoms. For example, in biology, evolution has selected metallatoporphyrin molecules in many vital biological processes involving electron transfer, oxygen transfer, and light harvesting.[3,4] In order to exploit porphyrins to translate these highly desirable functions to an interface, it is imperative that one understands the molecule−substrate interaction. Specifically, when dealing with reactive surfaces, the adsorption geometry, molecular conformation, and charge and spin state at the surface are critical in determining performance.

The study of the molecular conformation and the electronic structure of adsorbed porphyrin molecules using experimental techniques such as scanning tunneling microscopy (STM) and spectroscopy and electronic structure calculations such as density functional theory (DFT) calculations is an emerging field[5−9] and has mostly been concerned with weak adsorption on the coinage metals. In particular, the need for first principles calculations in order to better understand the electronic and geometric structure of adsorbed porphyrins has been recognized.[9]

However, it is generally difficult to determine the separate contributions of the macrocycle, the central metal atom if present, and any substituents on the adsorption characteristics of porphyrins. Specifically, since the central macrocycle is present in all porphyrins, understanding its interaction with an underlying substrate is of prime importance. We tackle this issue by studying the adsorption and bonding of the free-base porphine (H_2−P) onto a reactive Cu(110) surface using STM, reflection absorption infrared (IR) spectroscopy, and periodic DFT calculations. In our calculations, we have studied effects from nonlocal dispersion interactions, which become potentially important for large molecules, by using both a non-empirical van der Waals density functional (vdW-DF)[10−12] and a semilocal functional[13] for exchange and correlation effects. The adsorption of the free-base porphine (H_2−P) molecule on a metal surface provides an ideal system to investigate the contribution to the molecule−surface interaction from the macrocycle alone and has so far not been studied. This generic

* Address correspondence to mpersson@liv.ac.uk.

Received for review October 1, 2010 and accepted February 8, 2011.

Published online February 15, 2011
10.1021/nn102610k

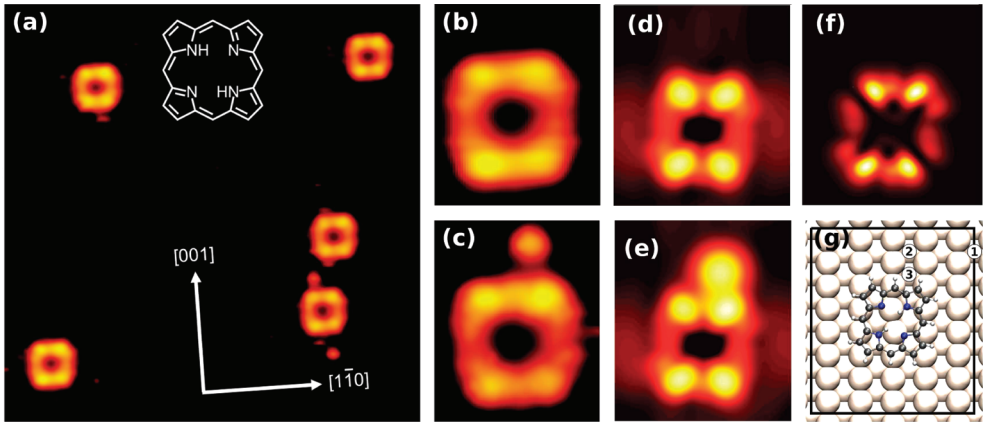

Figure 1. (a−c) Experimental STM images for a low coverage layer. The images are taken at −0.8 V and −0.4 nA: (a) 10 × 10 nm^2, (b,c) 1.3 × 1.6 nm^2, showing a single H_2−P molecule without and with an attached copper adatom, respectively. (d) Constant calculated integrated LDOS for H_2−P at short-bridge site on Cu(110) at −0.80 V, plotted between 5.9 and 6.8 Å above the top surface layer. (e) Constant calculated integrated LDOS for H_2−P and an adatom at position 2 on Cu(110), conditions as in (d). (f) LDOS arising from the LUMO and LUMO+1 of an isolated H_2−P molecule in vacuum, calculated at a constant height corresponding to 6 Å above the top surface layer. (g) Plot of the H_2−P molecule on Cu(110); the black box shows the 5 × 8 unit cell used in calculations, and the calculated copper adatom positions are indicated by the numbered circles.

molecule consists only of a macrocycle common to all porphyrin molecules and is both unsubstituted and metal-free. The macrocycle consists of four pyrrole rings connected through methine bridges and is both highly conjugated and aromatic with an electronic structure which can be readily altered by the addition of central metal atoms or peripheral substituents. Although STM images of unsubstituted metalloporphine molecules have previously been recorded,[14,15] they were measured on surfaces where the molecule−surface interaction is weak. To our knowledge, this is the first report of an adsorbed free-base porphine molecule with a strong molecule−surface interaction.

We are able to characterize both the adsorption geometry and the strong chemisorption bond: the former by total energy calculations and comparing STM images and IR spectra with simulated images, and the latter from the calculated electronic structure. Interestingly, the STM images also show that the molecules are able to capture copper adatoms, which is corroborated by our DFT calculations.

RESULTS AND DISCUSSION

Characterization from STM Images. Typical STM images of the adsorbed H_2−P molecule at submonolayer coverage are shown in Figure 1. The size and appearance of individual molecules in the STM images suggest that the H_2−P remain intact following deposition and are adsorbed with the plane of the molecule parallel to the surface. The edges of the molecule are aligned with the copper [001] and [1$\bar{1}$0] directions, and the molecules image as a bright ring with a dark depression in the center and four brighter protrusions within the ring. In addition to the bright rings corresponding to H_2−P molecules in STM images, occasionally, a bright protrusion is observed above or below the molecule in the [1$\bar{1}$0] direction, as shown in Figure 1c. Similar protrusions have been seen before for the adsorption of organic molecules on metal surface[16,17] and have been attributed to metal adatoms on the surface.

Although considerable insight can be gained from the STM experiments, several questions regarding the adsorption of H_2−P and its interaction with adatoms on the surface remain unanswered. STM experiments indicate largely planar adsorption; however, the exact adsorption site and geometry cannot be reliably determined. In addition, little information can be gained regarding the nature of the interaction between the molecule and the surface or between the molecule and copper adatoms present on the surface.

DFT Calculations. In order to investigate these outstanding issues, we carried out periodic DFT calculations of the adsorption site and geometry and STM images. Geometry optimization was performed starting from conformations with the center of the H_2−P molecule adsorbed above four different high symmetry sites on the Cu(110) surface and with the molecule aligned with the copper [001] and [1$\bar{1}$0] directions, as observed in experimental STM images. These four sites are the short-bridge (SB), top (T), hollow (H), and long-bridge (LB) sites. The resulting adsorption geometries are shown in Figure 2. Adsorption above the short-bridge site was found to be most stable with a significant adsorption energy of E_{ads} = 3.47(2.40) eV/molecule, where the value in the parentheses was obtained using GGA. Adsorption above T, H, and LB sites occurred significantly less favorably with E_{ads} of 2.88 (1.52), 2.69 (1.14), and 2.00 (0.21) eV/molecule, respectively. As shown by the GGA values in the parentheses, which does not include van der Waals interactions, GGA decreased the adsorption energies by about 1−2 eV compared to vdW-DF without changing the trend over the different sites. Furthermore, the vdW-DF gave only

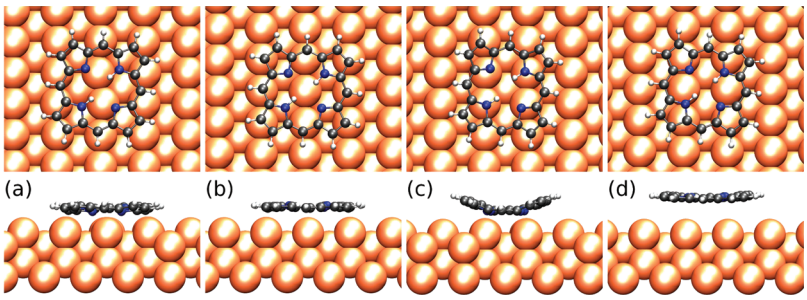

Figure 2. Calculated adsorption geometries with the center of the molecule above the (a) short-bridge, (b) on top, (c) hollow, and (d) long-bridge sites. The geometries are viewed along the [1$\bar{1}$0] rows (top panel) and from above (bottom panel). Copper atoms are shown as orange, carbon atoms as black, nitrogen atoms as blue circles, and hydrogen as white .

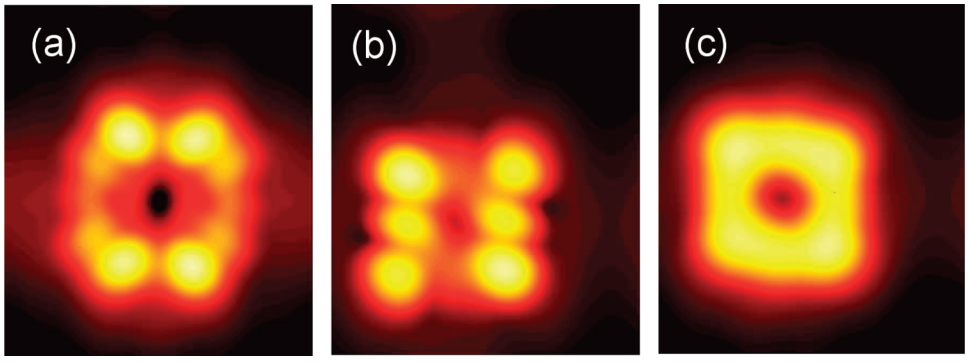

Figure 3. Calculated STM images of H_2−P in (a) on top (T), (b) hollow (H), and (c) long-bridge (LB) sites on Cu(110). The images were obtained from a constant, integrated LDOS at −0.80 V, plotted between 5.9 and (a) 6.8 Å and (b,c) 7.3 Å above the top surface layer under the same conditions as in Figure 1d.

rise to minor changes in the adsorption geometry. The average carbon−copper heights from vdW-DF are 2.20, 2.28, 2.58, and 3.30 Å for SB, T, H, and LB sites, respectively, decreased by less than 0.05 Å from the heights obtained by GGA.

A comparison of calculated images in Figure 3 and experimental STM image presented in Figure 1a shows that the H and LB sites can be ruled out. Both the simulated images in Figure 1d and Figure 3a for the SB and the T sites show four protrusions within a ring of higher tunneling current, two above and two below a central dark hole, in agreement with the experimental image. However, the clear energetic preference for the SB site suggests that this adsorption site is the experimentally observed one. Further support for this site comes from the analysis of the STM images of the molecule with attached adatoms presented below.

Strikingly, H_2−P is adsorbed very close to the corrugated Cu(110) surface. We find that, in the calculated lowest energy geometry, all atoms in the H_2−P molecule are placed between 1.9 and 2.65 Å above the top layer of copper atoms. These distances are much closer than would be expected for a physisorbed species, suggesting the formation of a chemisorption bond, in agreement with the fact that GGA gives E_{ads} = 2.40 eV/molecule, which is a large fraction of E_{ads} = 3.47 eV/molecule obtained using the vdW-DF. A strong molecule−substrate interaction is also shown by the substantial displacement of atoms in the copper substrate. In particular, the copper atoms near the center of the molecule are pulled toward the imminic nitrogen atoms (those not bonded to hydrogen) by 0.2 Å, which can be seen in Figure 1g and Figure 2a. In addition, upward displacements of 0.1 Å are observed for the four copper atoms beneath the corners of the molecule, and downward displacements of about 0.15 Å are observed for the second layer copper atoms directly beneath the molecule.

Infrared Vibrational Spectra. We obtained further information about the adsorption geometry and the molecule−surface interaction by performing RAIRS experiments and calculating a simulated RAIR spectrum. The experimental data are shown in Figure 4a, and the calculated spectrum shown in Figure 4b is in remarkably good agreement with experimental results, confirming that our calculated geometry and bonding corresponds closely to that found experimentally.

In both spectra, the strongest bands are observed at low frequencies between 700 and 800 cm^{-1}. The normal modes giving rise to these bands in the calculated spectrum are found to be out-of-plane hydrogen bending modes. Since vibrations with dynamic dipole moments normal to the molecular plane are the most active in RAIR spectra, the molecule must take up a largely planar adsorption geometry.[18] Low intensity absorption is observed in broad bands in the region of 1200−1400 cm^{-1}, which are due to vibrational modes with in-plane character. These may be active due to

small deviations away from planarity in the molecule, observable in Figure 2a, or due to coupling between in-plane modes and electronic degrees of freedom which is known to occur when a molecular orbital of an adsorbed molecule becomes partially occupied.[18] No significant absorption is seen at higher frequencies.

Analysis of the experimental IR spectrum of matrix isolated H_2−P suggests that the modes with the correct symmetry to be active in the RAIRS experiments should give rise to three strong bands at 691, 773−4, and 852 cm^{-1}.[19] This is indeed the case for RAIRS experiments on multilayers of H_2−P and calculations for molecules isolated in vacuum (see Supporting Information). However, at submonolayer coverages, the band at about 850 cm^{-1} is not observed and is replaced by one at about 740 cm^{-1}. This change must, therefore, arise from the interaction between the molecule and the surface, confirming that this interaction is significant.

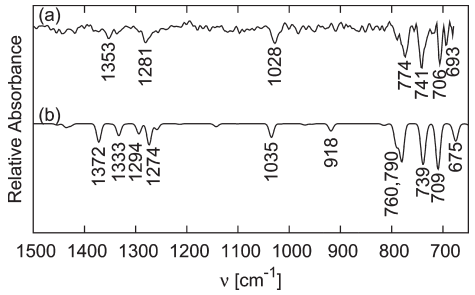

Figure 4. (a) Experimental RAIR spectrum of a low coverage of H_2−P adsorbed on Cu(110). The spectrum is plotted as reflectance $(R_0-R)/R_0$, where R_0 is the reflectance from the clean sample and R is the reflectance from the adsorbate covered sample. (b) Calculated RAIR spectrum for an H_2−P adsorbed on the short-bridge site of Cu(110). The calculated vibrational frequencies using the GGA and the vdW-DF differ by less than 2%. The bands are labeled with the frequencies of the corresponding normal modes.

Electronic Structure and Bonding. Using the DFT calculations, we were able to investigate the character of the electronic interaction between the surface and the porphine in considerable detail from the calculated electron density difference (EDD), projected density of states on molecular orbitals (MO-PDOS), and local density of states (LDOS). Our results for these characteristics of the electronic structure obtained using GGA are very similar to the ones obtained using vdW-DF (see Supporting Information).

The height dependence of the EDD shown in Figure 5c clearly shows a build up of electron density between the copper surface and the molecule. At the same time, the electron density is depleted near the plane of the molecule and at the top layer of the copper surface. This suggests that the interaction between the molecule and the surface has considerable covalent character. A cross section through the EDD at the height of maximum EDD (Figure 5a) shows that the increase in

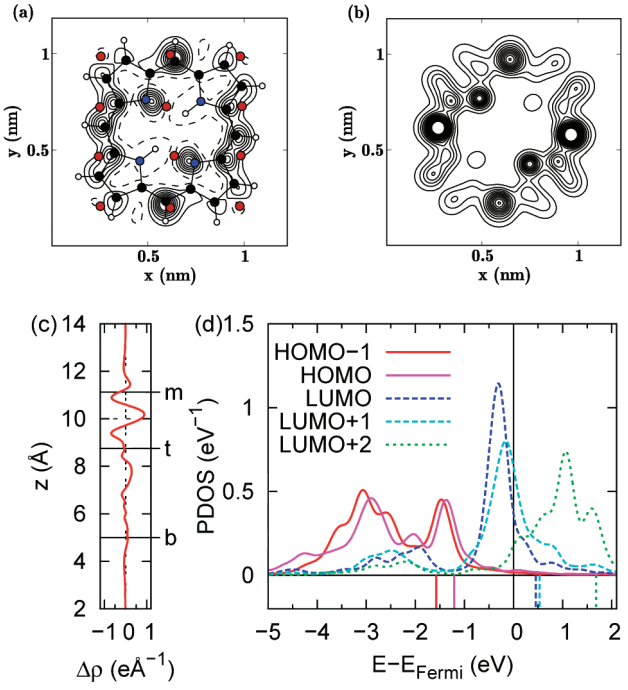

Figure 5. (a) Electron density difference taken at a constant height halfway between the surface and the molecule. Solid (dashed) lines are contours of electron accumulation (depletion) with a contour spacing of 0.01 $eÅ^{-3}$. (b) Electron density due to the LUMO and LUMO+1 orbitals, which has been calculated for the molecule in its adsorbed conformation but without the surface present. The density is plotted at the same height in the cell as in (a) and with the same contour levels. (c) Electron density difference integrated over the x and y directions. The heights of the bottom of the copper slab, b, the top of the copper slab, t, and the molecule, m, are shown. The horizontal dashed line shows the height used for the plot in (a) and (b). (d) Molecular orbital projected density of states. The vertical bars below show the calculated positions of the molecular orbitals in the absence of the copper surface. The vacuum energies of the systems with and without the copper surface present are aligned.

electron density is localized beneath most of the carbon atoms in the macrocycle and between the imminic nitrogen atoms and the copper surface atoms. The upward displacement of copper surface atoms is also localized in these areas, showing that they are the areas of strongest substrate−molecule attraction. Comparison of the cross section through the EDD with a cross section taken through the density of LUMO and LUMO+1 orbitals at the same height, calculated for the molecule in its adsorbed conformation but without the surface present (Figure 5b), clearly shows that the build up in electron density is due to donation into these two orbitals.

The donation of electron density into the previously unoccupied LUMO and LUMO+1 orbitals is also seen in the calculated MO-PDOS shown in Figure 5d. The corresponding MO-PDOS calculated in GGA are very similar to the vdW-DF results in Figure 4d (see Supporting Information). These orbitals both have π-character and are nearly degenerate for an isolated molecule. Following adsorption, these orbitals interact strongly with the copper surface, reflected by the broadening and splitting of the states in the MO-PDOS. They also become almost fully occupied, revealing a donation of electrons from the metal to the molecule. As a quantitative measure of the electron transfer, we have performed a Bader charge analysis[20] to partition the electron density of the full system between the molecule and the surface. This gives an overall transfer of 0.9 e^- to the H_2−P molecules from the surface. Therefore, as well as a covalent character, the chemisorption bond must also have a considerable ionic character.

The donation of electrons into the LUMO and LUMO+1 orbitals is experimentally supported by a comparison of the LDOS arising from both the LUMO and LUMO+1 orbitals of the isolated H_2−P subsystem in Figure 1f with the calculated and experimental STM images shown in Figure 1d and Figure 1b. The similarity between the LDOS arising from the LUMO and LUMO+1 orbitals calculated in vacuum and the STM images shows that the features in the STM images clearly arise from tunneling through states with LUMO and LUMO+1 character. Since STM images at negative biases represent tunneling from occupied states in the sample, this confirms that these orbitals become partially occupied following adsorption. In addition to the donation of electrons into the LUMO and LUMO+1 orbitals, a depletion of electron density is observed near the plane of the H_2−P molecule upon adsorption. This electron depletion may arise due to a back-donation of electrons from low energy σ-orbitals of the molecule to the copper substrate and explains why the calculated value of the electron transfer of 0.9 e^- is considerably smaller than the 4 e^- expected for a full occupation of the LUMO and LUMO+1 orbitals.

We have shown that a strong chemical interaction exists between H_2−P and the copper surface, in which electron transfer is found to take place into nearly degenerate unoccupied molecular orbitals with π-character. These results are in direct contrast to those calculated using a semilocal exchange-correlation functional for metalloporphines adsorbed on the Au(111) surface.[5] A weak interaction with an E_{ads} of 0.27 eV was found for Pd-porphine with no covalent bonding or charge transfer observed. Mn-porphine was found to interact more strongly with an E_{ads} of 0.80 eV. In this case, the molecule−substrate interaction was dominated by a transfer of electrons from the central manganese atom to the gold surface. In both cases, the interaction is considerably weaker than that calculated between H_2−P and copper and has a very different character. Similarly, a weak molecule−substrate interaction was found experimentally for Ni-porphine adsorbed on a silicon-supported silver surface.[14] The stronger molecule−substrate interaction between H_2−P and the Cu(110) is clearly very different from these previous examples of porphine adsorption and could have important implications for the alteration of the electronic structure of porphyrin molecules for use in certain applications. This molecule−substrate interaction is clearly not a pure physisorption interaction but rather a chemisorption interaction with short bonding distances, substantial substrate relaxations, and the vdW interactions are found to play a minor role using vdW-DF. We note that an accurate description of this latter interaction involving extended metal surfaces is still an active area of research. The vdW-DF has some shortcoming in describing bonding distances for pure physisorption systems[21] on metal surfaces. An alternative but empirical description of the vdW interaction is provided by DFT-D,[22,23] but its performance for extended metallic surfaces is not clear especially for short bonding distances. It is interesting to note that a molecule−substrate interaction with donation from the metal into unoccupied molecular π-orbitals, along with back-donation of electrons from the in-plane σ-orbitals of the molecule, was also recently described from DFT calculations of an organic molecule which is a strong electron acceptor, F4TCNQ, and was suggested to be a common feature of the bonding of organic electron acceptors with coinage metals.[24] The interaction of H_2−P with the Cu(110) surface would appear to have a similar character and provides experimental evidence that this is indeed a common feature of the bonding of such molecules to coinage metals.

Interactions with Adatoms. Calculations were also performed to confirm and investigate the capture and interaction of copper adatoms with H_2−P on the surface. In separate calculations, adatoms were placed in three different sites on the surface, shown in Figure 1g. Geometry optimizations were performed including the adatom, the molecule, and the top two layers of surface atoms. Taking the separated adatom and molecule

(site 1) as a reference, we found the configuration with an adatom on site 2 to be 57 (27) meV more stable, and with an adatom on site 3 proving less stable by 275 (222) meV. The values in the parentheses were obtained using GGA. Thus, the energetic preference for site 2 confirms that there exists a weak attractive interaction between H_2—P molecules and surface copper adatoms. There is a good agreement between the experimental STM image in Figure 1f and the integrated LDOS calculated with the adatom in position 2, confirming that a copper adatom in site 2 does give rise to a protrusion similar to that observed in experiment. At this site, the copper adatom is a surprisingly large distance from the molecule, at a distance of 3.7 Å from the closest molecular atoms.

The presence of metal adatoms on the surface and their interaction with adsorbed molecules have come under renewed interest recently due to the formation of ordered monolayers of metal-coordinated molecules on surfaces.[25] At room temperature, copper adatoms are known to be present and mobile on a Cu(110) surface and coordinate to carboxylate acid groups,[26,27] but free adatoms are not usually imaged by STM at this temperature due to their rapid diffusion. The diffusion of adatoms close to H_2—P molecules must therefore be reduced, presumably due to an increase of the energy barrier for these adatoms by their attractive interaction to the H_2—P molecules. From STM data, we can estimate the typical residing time of such attached adatoms and find it to be on the order of a few minutes. The protrusions are observed in off-center positions relative to the center of the molecules, and since copper adatoms are known to reside and diffuse preferentially in the troughs between the $[1\bar{1}0]$ rows,[16,28] this would suggest that the H_2—P molecules are adsorbed with their centers above a $[1\bar{1}0]$ row, in agreement with the results of our DFT calculations. Furthermore, the observed adatom—molecule distance is in better agreement with the SB site favored energetically by the DFT calculations than the T site.

Unfortunately, we cannot elucidate the character of the adatom—molecule interaction from the calculations. It is unlikely that there is a direct chemical interaction since the adatom is located 3.7 Å away from the closest molecular atoms. The most likely explanation is a substrate-mediated interaction between the molecule and the adatom through either conduction electrons or elastic interactions.[29] This weak interaction with the central porphyrin macrocycle is a new phenomenon, quite different from the direct chemical interaction with nitrogen-containing porphyrin substituents seen by Auwärter and coworkers.[17]

CONCLUSIONS

We have shown using scanning tunneling microscopy, reflection absorption infrared spectroscopy, and periodic density functional theory calculations using a non-empirical van der Waals density functional (vdW-DF) that a chemisorption bond is formed between the free-base porphyrin H_2—P molecule and a copper (110) surface. This bond involves predominantly a downward shift of nearly degenerate unoccupied molecular orbitals with π-character accompanied with a large electron transfer. A comparison with results obtained using a semilocal exchange-correlation functional (GGA) shows that the main effect of the nonlocal interactions provided by the vdW-DF is to increase the binding energy by about 40% for the most stable site with minor changes in the adsorption geometry and electronic structure. We believe that the described interaction should be present for many different substituted and metalated porphyrin molecules on the same surface and could also be relevant for chemisorption of such molecules on other reactive surfaces. This chemisorption is also expected to have an important influence on the molecular conformations especially for substituted molecules with potential implications for new physical and chemical properties not encountered for isolated molecules. Furthermore, a weak attractive interaction was also identified between H_2—P molecules and copper adatoms on the surface, which suggests that these complexes could act as potential precursors for the formation of organometallic nanostructures mediated by an interaction through copper adatoms at elevated temperatures.

EXPERIMENTAL AND THEORETICAL METHODS

Experiments were carried out at room temperature in different ultrahigh vacuum (UHV) chambers, one specifically designed for reflection absorption infrared spectroscopy (RAIRS), low energy electron diffraction (LEED), and temperature desorption spectroscopy and the others designed for STM using a SPECS Aarhus 150 instrument and LEED. Experimental details have been published elsewhere.[30] The Cu(110) single crystals were routinely cleaned by cycles of Ar^+ ion bombardment and annealing to 850 K, and the surface quality and purity were checked by LEED and STM. H_2—P (Frontiers Scientific) was used without further purification and deposited from a dedicated doser. During vacuum sublimation, the pressure in the main chamber typically stayed below 3×10^{-9} mbar.

Periodic DFT calculations were performed using the VASP code.[31] Plane waves were used as a basis set with an energy cutoff of 400 eV. Valence electron—core interactions were included using the projector augmented wave method.[32] Nonlocal dispersion interactions were included self-consistently using the non-empirical van der Waals density functional (vdW-DF) for the exchange-correlation effects developed by Langreth and Lundqvist.[10−12] In this functional, we used PBE exchange which is known to reduce the too strong repulsion of the original vdW-DF formulation, where revPBE is used. We also carried out structural optimization and total energy calculations

using the semilocal functional based on the generalized gradient approximation (GGA),[13] which omits any effects of the nonlocal interactions. All presented results are based on the vdW-DF if not stated otherwise. The Cu(110) surface was included as a four-layer slab in a supercell consisting of a 5 × 8 surface unit cell with a total height of 20.6 Å, and calculations were performed on a 3 × 2 × 1 *k*-point grid. During geometry relaxation calculations, the lowest two layers of copper atoms were held fixed, and the remaining atoms relaxed until the forces on them were less than 0.02 eV/Å.

Once the lowest energy conformation for the adsorbed H_2−P molecule was obtained, the adsorption energy, E_{ads}, was calculated by taking the difference between the sum of the total energies of the clean surface and the molecule without the surface present and the total energy of the full system. Calculations of the two subsystems were performed using the same unit cell and plane wave basis as for the full system, and a geometry relaxation was performed for each to find the lowest energy conformation before calculating E_{ads}.

When calculating the electron density difference (EDD), we performed calculations for the clean surface and the isolated molecule with their atoms held in the same position as in the total, fully relaxed system with the molecule adsorbed on the surface. The EDD was then calculated by taking the difference between the electron density of the full system and that of the two subsystems. The molecular orbital projected density of states (MO-PDOS) was calculated by projecting the orbitals of the isolated molecular subsystem onto those of the full system.

Calculated STM images were obtained following the Tersoff−Hamann approximation[33] by plotting contours of constant local density of states (LDOS), integrated from the Fermi energy to the given bias.[34] Since this method does not give absolute tunneling currents and the experimental tip−surface distance is not well-known, we chose a reasonable range of contours to plot with an average tip−surface distance of 6 Å. The high experimental tunneling resistance of 2 GΩ shows that experiments were performed with the tip far from chemical contact, and an average tip−surface distance of 6 Å avoids the region where the tip and sample interact chemically. The general features of the calculated image are retained upon increasing the average tip−surface distance to 10 Å, but the resolution and corrugation of the image are reduced.

For a comparison of the data of the RAIRS experiment, we calculated the normal modes for the adsorbed molecule in its lowest energy configuration using the harmonic approximation by diagonalizing the force constant matrix. This matrix was constructed using finite differences of calculated forces, by displacing the atoms in the adsorbed H_2−P molecule. At the same time, we calculated the change in the dipole moment normal to the surface for each mode and used it to simulate the results of experimental data.

Acknowledgment. M.P. thanks the Marie Curie Research Training Network PRAIRIES, Contract MRTN-CT-2006-035810, and the Swedish Research Council (VR) for financial support, M.S.D. the University of Liverpool (UoL) for funding of postdoctoral fellowship, A.R. and R.R. the EU network TANSAS. Computational resources provided by UoL and SNAC are also acknowledged.

Supporting Information Available: Extended set of figures: an experimental reflection absorption infrared spectrum of a multilayer of H_2−P and a calculated infrared spectrum of the molecule in vacuum and calculated density of states projected on molecular orbitals using the GGA. This material is available free of charge *via* the Internet at http://pubs.acs.org.

REFERENCES AND NOTES

1. Jurow, M.; Schuckman, A. E.; Batteas, J. D.; Drain, C. M. Porphyrins as Molecular Electronic Components of Functional Devices. *Coord. Chem. Rev.* **2010,** *254*, 2297–2310.
2. Mohnani, S.; Bonifazi, D. Supramolecular Architectures of Porphyrins on Surfaces: The Structural Evolution from 1D to 2D to 3D to Devices. *Coord. Chem. Rev.* **2010,** *254*, 2342–2362.
3. Groves, J. T. The Bioinorganic Chemistry of Iron in Oxygenases and Supramolecular Assemblies. *Proc. Natl. Acad. Sci. U.S.A.* **2003,** *100*, 3569.
4. Woggon, W.-D. Metalloporphyrines as Active Site Analogues: Lessons from Enzymes and Enzyme Models. *Acc. Chem. Res.* **2005,** *38*, 127.
5. Leung, K.; Rempe, S. B.; Schultz, P. A.; Sproviero, E. M.; Batista, V. S.; Chandrosa, M. E.; Medforth, C. J. Density Functional Theory and DFT+U Study of Transition Metal Porphines Adsorbed on Au(111) Surfaces and Effects of Applied Electric Fields. *J. Am. Chem. Soc.* **2006,** *128*, 3659–3668.
6. Wende, H..;*et al.*Substrate-Induced Magnetic Ordering and Switching of Iron Porphyrin Molecules. *Nat. Mater.* **2007,** *6*, 516–520.
7. Zotti, L.; Teobaldi, G.; Hofer, W.; Auwärter, W.; Weber-Bargioni, A.; Barth, J. *Ab-Initio* Calculations and STM Observations on Tetrapyridyl and Fe(II)-Tetrapyridyl-Porphyrin Molecules on Ag(111). *Surf. Sci.* **2007,** *601*, 2409–2414.
8. Auwärter, W.; Weber-Bargioni, A.; Brink, S.; Riemann, A.; Schiffrin, A.; Ruben, M.; Barth, J. V. Controlled Metalation of Self-Assembled Porphyrin Nanoarrays in Two Dimensions. *ChemPhysChem* **2007,** *8*, 250–254.
9. Weber-Bargioni, A.; Auwärter, W.; Klappenberger, F.; Reichert, J.; Lefrançois, S.; Strunskus, T.; Wöll, C.; Schiffrin, A.; Pennec, Y.; Barth, J. V. Visualizing the Frontier Orbitals of a Conformationally Adapted Metalloporphyrin. *ChemPhysChem* **2008,** *9*, 89–94.
10. Dion, M.; Rydberg, H.; Schröder, E.; Langreth, D. C.; Lundqvist, B. I. Van derWaals Density Functional for General Geometries. *Phys. Rev. Lett.* **2004,** *92*, 246401.
11. Dion, M.; Rydberg, H.; Schröder, E.; Langreth, D. C.; Lundqvist, B. I. Erratum: Van der Waals Density Functional for General Geometries [Phys. Rev. Lett. 92, 246401 (2004)]. *Phys. Rev. Lett.* **2005,** *95*, 109902(E).
12. Langreth, D. C..;*et al.*A Density Functional for SparseMatter. *J. Phys.: Condens. Matter* **2009,** *21*, 084203.
13. Perdew, J. P.; Chevary, J. A.; Vosko, S. H.; Jackson, K. A.; Pederson, M. R.; Singh, D. J.; Fiolhais, C. Atoms,Molecules, Solids, and Surfaces: Applications of the Generalized Gradient Approximation for Exchange and Correlation. *Phys. Rev. B* **1992,** *46*, 6671–6687.
14. Beggan, J. P.; Krasnikov, S. A.; Sergeeva, N. N.; Senge, M. O.; Cafolla, A. A. Self-Assembly of Ni(II) Porphine Molecules on the Ag/Si(111)-($\sqrt{3}\times\sqrt{3}$)R30° Surface Studied by STM/STS and LEED. *J. Phys.: Condens. Matter* **2008,** *20*, 015003.
15. Yoshimoto, S.; Inukai, J.; Tada, A.; Abe, T.; Morimoto, T.; Osuka, A.; Furuta, H.; Itaya, K. Adlayer Structure of and Electrochemical O_2 Reduction on Cobalt Porphine-Modified and Cobalt Octaethylporphyrin-Modified Au(111) in $HClO_4$. *J. Phys. Chem. B* **2004,** *108*, 1948–1954.
16. Böhringer, M.; Schneider, W. D.; Glöckler, K.; Umbach, E.; Berndt, R. Adsorption Site Determination of PTCDA on Ag(110) by Manipulation of Adatoms. *Surf. Sci.* **1998,** *419*, L95–L99.
17. Auwärter, W.; Klappenberger, F.; Weber-Bargioni, A.; Schiffrin, A.; Strunskus, T.; Woll, C.; Pennec, Y.; Riemann, A.; Barth, J. V. Conformational Adaptation and Selective Adatom Capturing of Tetrapyridyl-Porphyrin Molecules on a Copper (111) Surface. *J. Am. Chem. Soc.* **2007,** *129*, 11279–11285.
18. Tautz, F. S.; Sloboshanin, S.; Shklover, V.; Scholz, R.; Sokolowski, W.; Schaefer, J. A.; Umbach, E. Substrate Influence on the Ordering of Organic Submonolayers: A Comparative Study of PTCDA on Ag(110) and Ag(111) Using HREELS. *Appl. Surf. Sci.* **2000,** *166*, 363–369.
19. Radziszewski, J. G.; Nepras, M.; Balaji, V.; Waluk, J.; Vogel, E.; Michl, J. Polarized Infrared Spectra of Photooriented Matrix-Isolated Free-Base Porphyrin Isotopomers. *J. Phys. Chem.* **1995,** *99*, 14254–14260.
20. Tang, W.; Sanville, E.; Henkelman, G. A Grid-Based Bader Analysis Algorithm without Lattice Bias. *J. Phys.: Condens. Matter* **2009,** *21*, 084204.
21. Toyoda, K.; Hamada, I.; Lee, K.; Yanagisawa, S.; Morikawa, Y. Density Functional Theoretical Study of Pentacene/Noble

Metal Interfaces with van der Waals Corrections: Vacuum Level Shifts and Electronic Structures. *J. Chem. Phys.* **2010,** *132*, 134703–9.
22. Grimme, S. Semiempirical GGA-Type Density Functional Constructed with a Long-Range Dispersion Correction. *J. Comput. Chem.* **2006,** *27*, 1787–1799.
23. Grimme, S.; Antony, J.; Ehrlich, S.; Krieg, H. A Consistent and Accurate *Ab Initio* Parametrization of Density Functional Dispersion Correction (DFT-D) for the 94 Elements H-Pu. *J. Chem. Phys.* **2010,** *132*, 154104–19.
24. Rangger, G. M.; Hofmann, O. T.; Romaner, L.; Heimel, G.; Broker, B.; Blum, R.-P.; Johnson, R. L.; Koch, N.; Zojer, E. F4TCNQ on Cu, Ag, and Au as Rototypical Example for a Strong Organic Acceptor on Coinage Metals. *Phys. Rev. B* **2009,** *79*, 165306–12.
25. Barth, J. V. Fresh Perspectives for Surface Coordination Chemistry. *Surf. Sci.* **2009,** *603*, 1533–1541.
26. Perry, C. C.; Haq, S.; Frederick, B. G.; Richardson, N. V. Face Specificity and the Role of Metal Adatoms in Molecular Reorientation at Surfaces. *Surf. Sci.* **1998,** *409*, 512–520.
27. Dougherty, D. B.; Maksymovych, P.; Yates, J. T., Jr. Direct STM Evidence for Cu-Benzoate Surface Complexes on Cu(110). *Surf. Sci.* **2006,** *600*, 4484–4491.
28. Yildirim, H.; Kara, A.; Durukanoglu, S.; Rahman, T. S. Calculated Pre-exponential Factors and Energetics for Adatom Hopping on Terraces and Steps of Cu(100) and Cu(110). *Surf. Sci.* **2006,** *600*, 484–492.
29. Bogicevic, A.; Ovesson, S.; Hyldgaard, P.; Lundqvist, B. I.; Brune, H.; Jennison, D. R. Nature, Strength, and Consequences of Indirect Adsorbate Interactions on Metals. *Phys. Rev. Lett.* **2000,** *85*, 1910.
30. Robin, A..;*et al.*Adsorption and Organization of the Organic Radical 3-Carboxyproxyl on a Cu(110) Surface: A Combined STM, RAIRS, and DFT Study. *J. Phys. Chem. C* **2009,** *113*, 13223–13230.
31. Kresse, G.; Furthmüller, J. Efficient Iterative Schemes for *Ab Initio* Total-Energy Calculations Using a Plane-Wave Basis Set. *Phys. Rev. B* **1996,** *54*, 11169–11186.
32. Kresse, G.; Joubert, D. From Ultrasoft Pseudopotentials to the Projector Augmented-Wave Method. *Phys. Rev. B* **1999,** *59*, 1758–1774.
33. Tersoff, J.; Hamann, D. R. Theory and Application for the Scanning Tunneling Microscope. *Phys. Rev. Lett.* **1983,** *50*, 1998–2001.
34. Sacks, W.; Gauthier, S.; Rousset, S.; Klein, J.; Esrick, M. A. Surface Topography in Scanning Tunneling Microscopy: A Free-Electron Model. *Phys. Rev. B* **1987,** *36*, 961–967.